# *TI Designs：TIDA-01588*
# *效率大于 90% 且适用于有刷直流伺服驱动器的 10.8V/15W 2.4cm² 功率级参考设计*

## 说明

此 15W 12mm x 20mm 功率级参考设计用于驱动和控制依靠三至六芯锂离子电池供电运行的有刷直流 (BDC) 电机的位置。此解决方案经过优化，效率高，外形尺寸极小，可轻松适应电机，实现精确的电机位置控制。此设计还能高速驱动电机，不提供任何位置反馈。本参考设计演示了快速精确的电流检测，实现出色的扭矩控制，且板载 MCU 提供 UART 连接，从而支持通过外部控制器进行控制。

## 资源

| | |
|---|---|
| TIDA-01588 | 设计文件夹 |
| DRV8870 | 产品文件夹 |
| MSP430FR2433 | 产品文件夹 |
| TLV9061 | 产品文件夹 |
| TPS709 | 产品文件夹 |
| TVS3300 | 产品文件夹 |
| ESD122 | 产品文件夹 |

TI E2E™ Community — 咨询我们的 E2E™ 专家

## 特性

- 有刷直流伺服驱动器的工作电压范围为 6.5V 至 25.2V（3 至 6 节锂离子电池）
- 支持 1.4A RMS 连续电机绕组电流和 2.75A 峰值电机绕组电流
- 使用编码器或电位计位置反馈实现精确的电机位置控制
- 12mm × 20mm 的极小型 PCB 外形尺寸
- 电流检测的校准精度误差低于 1%，可实现精确的电机扭矩控制
- 功率级效率高达 90% 以上，无需散热器
- 过流、击穿、过电压和过热保护
- 提供 UART 有线通信
- 工作环境温度：–20°C 至 55°C
- 高度集成的高效电机驱动器的使用减少了总体 BOM，实现了小巧的 PCB 外形，减少了冷却负荷量

## 应用

- 类人机器人
- 扫地机器人
- 割草机器人

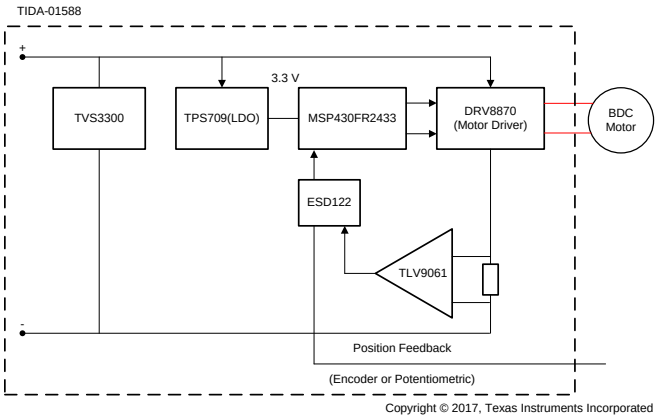




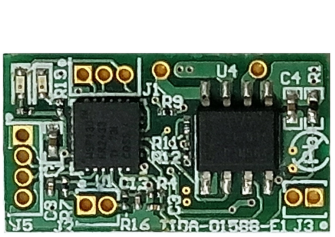

# 1 System Description

A humanoid robot is a type of service robot used in wide-end applications, such as research applications where human access is risky, high-end toys used for teaching, dancing, and speaking, and more. Multiple motors are present in a typical humanoid depending upon the features and application requirement. The commonly used motors are BDC, brushless DC (BLDC), and sometimes stepper types. 图 1 shows the examples of motor drive locations in a typical humanoid. The high-end or high-power motors are typically present in the neck, legs, shoulders, and so on. Low-end or low-power motors are used in other locations such as elbows, knees, fingers, and so on Low-end motors normally use BDC motors with power levels less than 15 W. The electronic drive used in these motors has the following requirements:

- Must be small enough to fit with the motor
- Must support accurate position and torque control
- Must have the sufficient holding torque capability

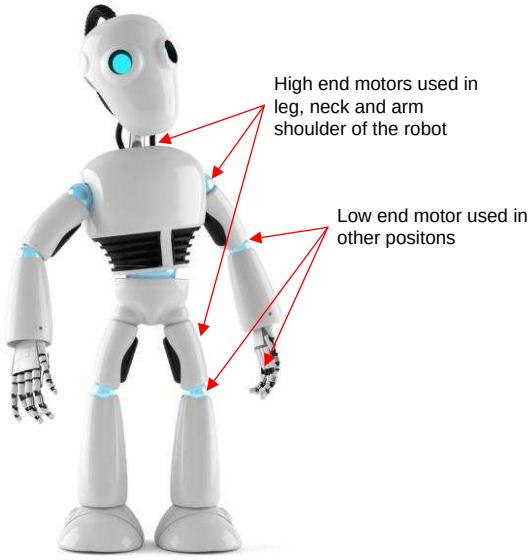


**图 1. Typical Humanoid—Motor Drive Locations**

Vacuum robots are another service robot widely used in consumer applications for cleaning. The motors used in vacuum robots have different requirements like high-speed rotation, high torque-slow speed operation, or position control depending on the functionality these motors support (for example, suction, wheel, side brush, position control of the robotic vision control motor, and so on). BDC, BLDC, or stepper motors are typically used. The electronic drives have similar requirements as said in the case of humanoids.

This reference design can support the position control in a humanoid or the motor control in a vacuum robot. The design demonstrates the BDC motor servo drive power stage in a very small form factor using the highly-integrated motor driver DRV8870 featuring a low $R_{DS(ON)}$ of 565 mΩ (HS+LS), in a 4.9-mm × 6-mm package. The device features integrated current regulation and protection features, which enables the reduction of overall BOM. The thermal PowerPAD™ integrated circuit package eases the heat dissipation to the PCB. The TPS709 LDO features a low-quiescent current (<1 μA) and generates the low-noise,

stable, 3.3-V power supply for the MCU. The TLV9061 amplifier enables accurate current sensing for precise torque control, and the small package allows over all PCB form factor reduction. The MSP430FR2433 runs the position control algorithm by taking the position feedback signals from the motor. The ESD122 and the TVS3300 provide ESD and surge voltage protection on different voltage lines.

The test report evaluates the board power capability, efficiency, current sensing accuracy, overcurrent protection, peak current capability, and the position control with sufficient hold up torque.

## 1.1 Key System Specifications

表 1. Key System Specifications

| PARAMETERS | SPECIFICATIONS |
|---|---|
| Input voltage | 10.8-V DC (6.5-V minimum to 25.2-V maximum) |
| Rated output power | 15 W |
| RMS winding current | 1.4 A |
| Peak winding current | 2 A (for 2 s), 2.75 A (for 1 s) |
| Power stage switching frequency | 20 kHz (adjustable) |
| Feedback signals | DC bus voltage, encoder or potentiometric position feedback, low-side DC bus current |
| Protections | Overcurrent, input undervoltage, overtemperature, shoot-through |
| Cooling | Natural cooling only, no heat sink |
| Operating ambient | –20°C to 55°C |
| Board specification | 12-mm x 20-mm, 2-layer, 1-oz copper, 1.6-mm board thickness |
| Efficiency | > 90% |

# 2 System Overview

## 2.1 Block Diagram

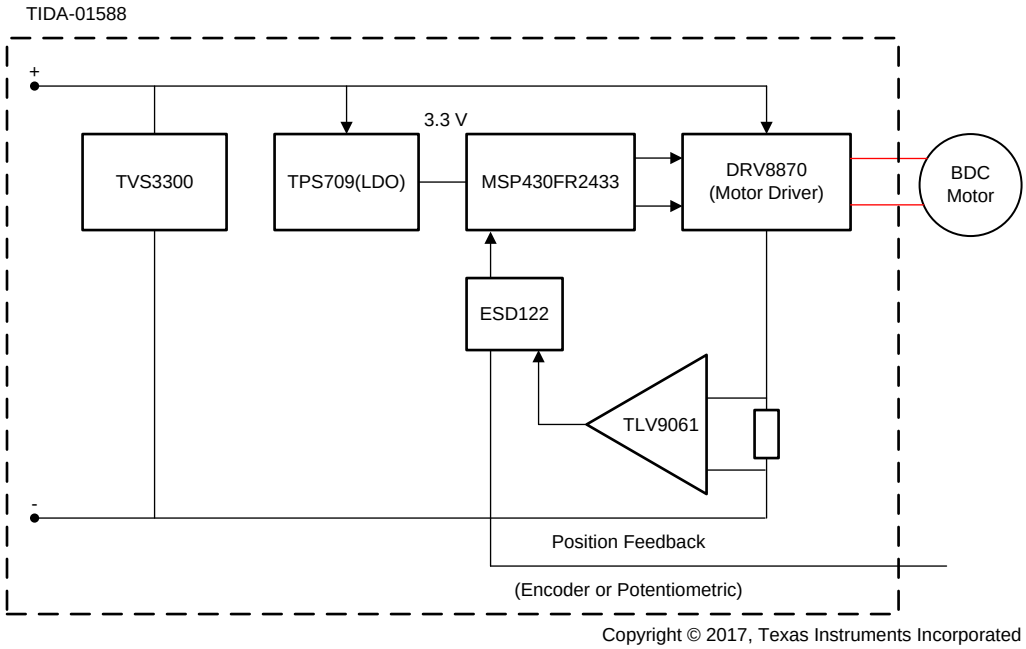




图 **2. TIDA-01588 Block Diagram**

## 2.2 Highlighted Products

### 2.2.1 DRV8870

The key requirements in selecting the motor driver are:

- Small chip size BDC motor driver (full bridge) with high level of integration and protection
- Support 1.5-A RMS continuous and 3-A peak
- Minimal power loss and good heat dissipation

The reference design uses the highly-integrated BDC motor driver DRV8870. Two logic inputs control the H-bridge driver, which consists of four N-channel MOSFETs that can control motors bidirectionally with up to 3.6-A peak current. The inputs can be pulse-width modulated (PWM) to control motor speed using a choice of current-decay modes. Setting both inputs low enters the driver into a low-power sleep mode.

The DRV8870 device features integrated current regulation based on the analog input VREF and the voltage on the ISEN pin, which is proportional to motor current through an external sense resistor. The ability to limit current to a known level can significantly reduces the system power requirements and bulk capacitance required to maintain stable voltage especially for motor startup and stall conditions. The device is fully protected from faults and short circuits including undervoltage (UVLO), overcurrent (OCP), and overtemperature (TSD). When the fault condition is removed, the device automatically resumes normal operation.

### 2.2.2 MSP430FR2433

The MSP430FR2433 microcontroller (MCU) is part of the MSP430™ MCU value line sensing portfolio, TI's lowest-cost family of MCUs. The architecture, FRAM, and integrated peripherals, combined with extensive low-power modes, are optimized to achieve extended battery life in portable and battery-powered applications in a small VQFN package (4 mm × 4 mm). FRAM technology combines the low-energy fast writes, flexibility, and endurance of RAM with the non-volatility of flash.

The MSP430FR2433 has MCU configurations with two 16-bit timers, two universal serial communication interfaces (USCIs), a 32-bit hardware multiplier and a high-performance 10-bit 200-ksps analog-to-digital converter (ADC). The device is capable of working up to a clock frequency of 16 MHz. The ports 1 and 2 of the MSP430FR2433 have interrupt capabilities.

The availability of required peripherals in a small package along with the low-power consumption makes the device ideal for a battery-powered motor drive application in service robots.

### 2.2.3 TLV9061

The TLV9061 (single), TLV9062 (dual), and TLV9064 (quad) are single-, dual-, and quad- low-voltage (1.8 V to 5.5 V) operational amplifiers (op amps) with rail-to-rail input- and output-swing capabilities. These devices are highly cost-effective solutions for applications where low-voltage operation, small footprint, and high-capacitive load drive are required. Although the capacitive load drive of the TLV9061 is 100 pF, the resistive open-loop output impedance makes stabilizing with higher-capacitive loads simpler. The TLV9061 has a single rail supply, low quiescent current (568 μA), unity gain bandwidth of 10 MHz. The TLV906x family helps to simplify system design because the family is unity-gain stable, integrates the RFI and EMI rejection filter, and provides no phase reversal in overdrive condition.

Micro-size packages, available down to 0.8 mm × 0.8 mm, help the designer to achieve very small form factor.

### 2.2.4 TPS709

The TPS70933 linear regulator is an ultra-low quiescent current device designed for power-sensitive applications. The LDO can work up to a 30-V input voltage, which makes it ideal for up to six-cell Li-ion battery supply application. A precision band-gap and error amplifier provides 2% accuracy over temperature. A quiescent current of only 1 μA makes this LDO ideal for battery-powered, always-on systems that require very little idle-state power dissipation. This device has thermal-shutdown, current limit, and reverse-current protections for added safety. The TPS70933 linear regulator is available in WSON-6 and SOT-23-5 packages.

### 2.2.5 TVS3300

The TVS3300 is a transient voltage suppressor that provides robust protection for electronic circuits exposed to high-transient voltage events. Unlike a traditional TVS diode, the TVS3300 precision clamp triggers at a lower breakdown voltage and regulates to maintain a flat clamping voltage throughout a transient overvoltage event. The lower clamping voltage combined with a low dynamic resistance enables a unique TVS protection solution that can lower the voltage a system is exposed during a surge event by up to 30% in unidirectional configuration and up to 20% in bidirectional configuration when compared to traditional TVS diodes.

The TVS3300 is a unidirectional precision surge protection clamp with a 33-V working voltage designed specifically to protect systems with mid-voltage rails in industrial, communication, and factory automation applications. The TVS3300 has a fast response time when surge current is applied, so there is no overshoot voltage during clamping, which makes the device ideal to replace traditional TVS and zener diodes.

The TVS3300 is available in two small footprint packages that can reduce footprint by 94% (WCSP package) and 79% (SON package) for space-constrained applications when used in place of an industry standard SMB package. Both package options robustly dissipate the surge power and provide up to 58% lower leakage current compared to traditional TVS diodes in SMA and SMB package.

### 2.2.6 ESD122

The ESD122 is a bidirectional TVS ESD protection diode array. The ESD122 is rated to dissipate contact ESD strikes at the maximum level specified in the IEC 61000-4-2 international standard (17-kV contact, 17-kV air-gap). This device features a low I/O capacitance per channel. The low-dynamic resistance and low-clamping voltage ensure system level protection against transient events.

## *2.3 System Design Theory*

### 2.3.1 DC Voltage Input to Board

The board gets the DC input voltage through the jumper J3. The TVS3300 is a surge protection clamp provided at the input to protect the circuit from input voltage surges. The design is optimized for a three-cell Li-ion battery and can support up to six-cell applications with a maximum voltage of 25.2 V.

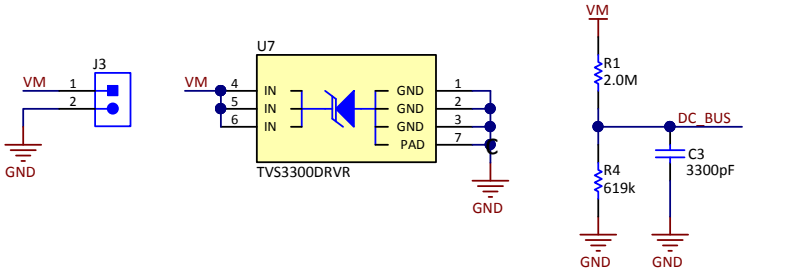




图 **3. Schematic of Battery Power Input Section**

The input supply voltage VM is scaled using the resistive divider network, which consists of R1, R4, and C3, and is fed to the MCU. Considering the maximum voltage for the MCU, ADC input is 3.3 V, and the maximum DC input voltage measurable by the MCU is calculated as 公式 1.

$$V_{DC}^{max} = V_{ADC\_DC}^{max} \times \frac{(619\ k\Omega + 2000\ k\Omega)}{619\ k\Omega} = 3.3 \times \frac{(619\ k\Omega + 2000\ k\Omega)}{619\ k\Omega} = 13.96\ V \quad (1)$$

Considering a 10% headroom for this value, the maximum recommended voltage input to the system is 13.96 × 0.9 = 12.56 V. For a power stage operating from three-cell Li-ion with a maximum operating voltage of 12.6 V, this voltage feedback resistor divider is ideal. Also, this choice gives optimal ADC resolution for a system operating from 6 V to 12.6 V.

注: Adjust the value of R4 for supporting the voltage sensing up to 25.2-V input voltage. For example select R4 = 309 k to support up to 25.2 V.

### 2.3.2 DRV8870—BDC Motor Driver

图 4 shows the schematic of the DRV8870 motor driver. The DRV8870 device is made of four N-channel MOSFETs that can control motors bidirectionally with up to 3.6-A peak current.

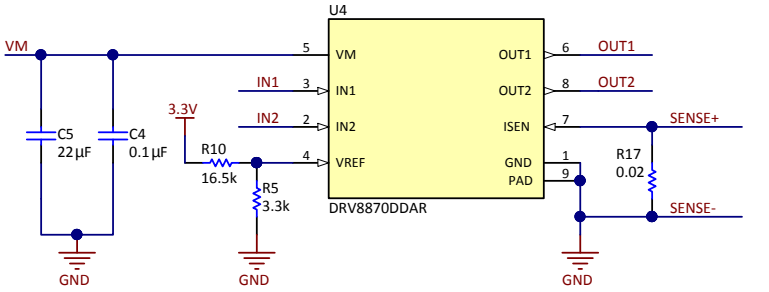




图 4. Schematic of DRV8870-BDC Motor Driver

A 22-µF capacitor (C5) is used as the VM input bulk capacitor. Another 0.1-µF bypass capacitor (C4) is also provided. C5 and C4 are selected to support up to 25.2 V. IN1 and IN2 are the PWM inputs from the MCU, which control the half-bridge MOSFETs. OUT1 and OUT2 are the phase node of the H-bridge, which must be connected to the external BDC motor winding.

The sense resistor (R17) is chosen appropriately for sensing the H-bridge low-side current. The sense resistor R17 along with voltage at the VREF pin of DRV8870 decides the internal peak current limit of DRV8870. The voltage across R17 is also fed to the current sense amplifier circuit (described in 节 2.3.4) to monitor the motor current precisely.

The DRV8870 device limits the output current based on the analog voltage input at VREF, and the external sense resistor R17 on the ISEN pin according to 公式 2.

$$I_{TRIP}(A) = \frac{VREF\,(V)}{A_V \times R_{ISEN\,(\Omega)}} = \frac{VREF\,(V)}{10 \times R_{ISEN\,(\Omega)}} \quad (2)$$

Resistors R10 (16.5 kΩ) and R5 (3.3 kΩ) generate an appropriate reference voltage (VREF) of 0.55 V. The 0.02-Ω sense resistor (R17) and VREF of 0.55 V fixes a peak current limit of 2.75 A per 公式 2.

### 2.3.3 Sense Resistor Selection

The selection of sense resistor depends on different factors as follows:

- Required peak current limit from DRV8870 along with VREF pin voltage of DRV8870
- Power dissipation in the sense resistor
- Offset error voltage and gain of the current sense amplifier

The sense resistors are designed to carry a continuous nominal RMS current of 1.5 A and a peak current of 2.75A. A high-sense resistance value increases the power loss in the resistors. A low-sense resistor value increases the error due to input offset voltage of the current sense amplifier at high gain. If the current-sense amplifier is used without offset calibration, select the sense resistor value, so the sense voltage across the resistor is sufficiently higher than the op-amp input offset voltage, which reduces the effect of the offset error. The TLV9061 has a typical input offset error voltage of 0.3 mV (maximum of 1.6 mV). The reference design uses 0.02-Ω sense resistor, and the power loss in sense resistor can be calculated as in 公式 3.

$$\text{Power loss in the resistor} = I_{RMS}^{2} \times R_{SENSE} = 1.5^{2} \times 0.02 = 0.045\ W \quad (3)$$

Using 公式 3 at 2.75-A peak current, the power loss in the resistor = 0.151 W (for 1 second)

### 2.3.4 Current Sense Amplifier

The TLV9061 is used as an external current sense amplifier because of small form factor, good gain bandwidth product (GBW), good slew rate, input EMI filters, rail to rail operation, power supply voltage range, and low offset voltage. This reference design uses the differential amplifier configuration shown in 图 5 with a gain of 24.95 V/V (adjustable with different feedback resistor values). The current is sensed at the DC supply return path, which is normally unidirectional. The current can be bidirectional under regenerative mode support. The bidirectional current sensing is made possible by adding a level shift ($V_{REF}$) of approximately 1.2 V using the resistors R11 and R12.

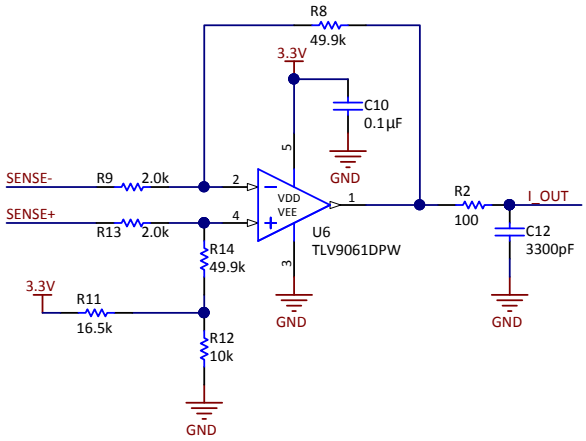




图 5. TLV9061 Current Sense Amplifier Schematic

注: For accurate voltage level shifting, a reference voltage IC or an op-amp voltage follower circuit can be used to generate the 1.2 V.

The current sense resistor of 20 mΩ, amplifier gain of 24.95, and the level shift of approximately 1.2 V make the amplifier circuit measure the current accurately from –2-A to 3.5-A peak. The output voltage of the amplifier can be approximately calculated using 公式 4.

$$V_{OUT} = V_{REF} + (I \times CSA\_GAIN \times R_{ISEN}) \quad (4)$$

The output of the op amp connects to the MCU through the output low-pass filter R2 and C12.

Consider connecting a 0.01-µF ceramic capacitor across the resistor R12 for a noise-free level-shift reference voltage for the op amp and connecting a low-pass filter after the sense resistor and before the amplifier input depending on the layout used.

### 2.3.5 LDO—3.3-V Generation

The reference design uses the ultra-low quiescent current, LDO linear regulator TPS70933 to generate the 3.3-V power supply for the MCU from the input voltage of 10.8 V. 图 6 shows the schematic of the LDO circuit.

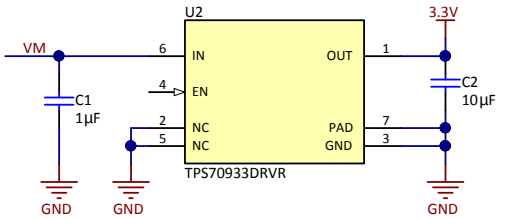




图 **6. Schematic of 3.3-V LDO**

The selection of LDO depends on the wide input voltage support (in this design, from 6.5 V to 25.2 V), the load current, and power dissipation. Power dissipation depends on input voltage and load conditions. Power dissipation ($P_{diss}$) is equal to the product of the output current and the voltage drop across the output pass element, as shown in 公式 5.

$$P_{diss} = (V_{IN} - V_{OUT}) \times I_{OUT} \quad (5)$$

Assuming a nominal LDO load current of 20 mA, the power dissipation at $V_{IN}$ = 25.2 V can be calculated as: $P_{diss}$ = (25.2 – 3.3) × 0.02 = 0.438 W. 表 2 shows the specifications of the LDOs used in this reference design. At lower input voltage, the power dissipation in the LDO reduces. This reference design assumes a maximum LDO output current of 30 mA when operating from three-cell Li-ion battery.

表 **2. Specification of Buck Converter**

| PARAMETER | DESIGN SPECIFICATION |
|---|---|
| Input voltage | 6 V to 25.2 V (10.8-V nominal) |
| Output voltage | 3.3 V |
| Maximum output current | 30 mA (at 10.8 V input voltage) |

### 2.3.6 MCU—MSP430FR2433

图 7 shows the configuration of the MSP430FR2433 MCU. The reference design uses 4.7-µF decoupling capacitor (C6). A 0.1-µF capacitor is added to obtain the best performance at a high frequency. The timer A module of the MCU is used for PWM generation. The pin TA0.1 and TA0.2, which generated the necessary PWM output signals, are connected to IN1 and IN2 of the DRV8870. All feedback signals including DC bus voltage, potentiometric analog voltage position feedback, and current sense amplifier output are each mapped to a 10-bit ADC channel of the MCU. The encoder position feedback is connected to the GPIO pins of the MCU, and those GPIO pins are configured for port interrupt on edges. This configuration enables the proper counting of encoder pulses and allows accurate position sensing. The signals TEST and RST are connected to the programming connector. The provision for UART communication is enabled through the pins RXD and TXD.

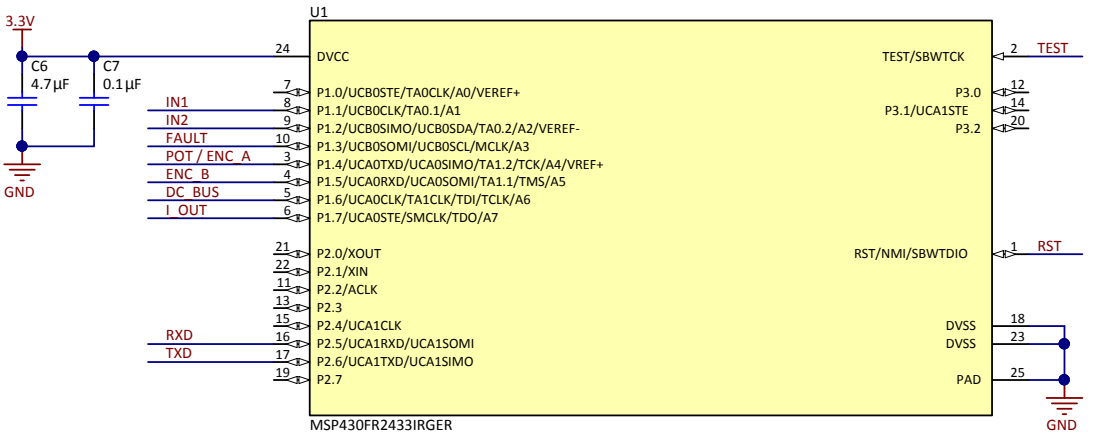




**图 7. MSP430FR2433 Schematic**

### 2.3.7 Encoder or Potentiometric Position Feedback

图 8 shows the position feedback interface from the motor to the reference design board. The reference design can support encoder position feedback or a potentiometric analog voltage position feedback. The power supply is 3.3 V for both cases.

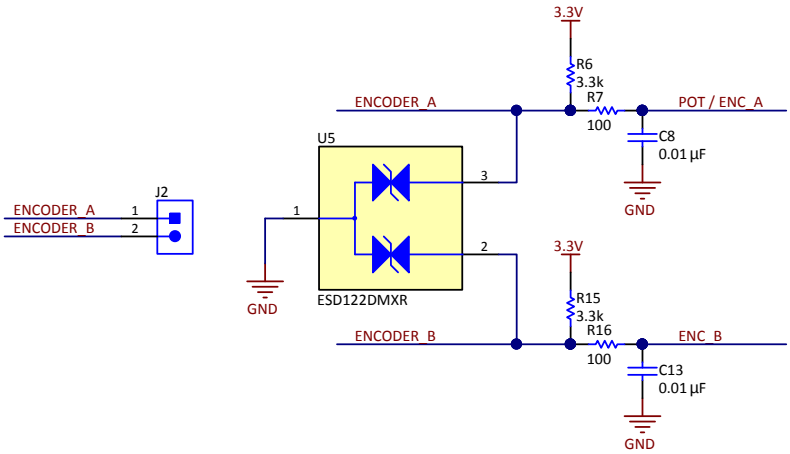


**图 8. Motor Position Feedback Schematic**

The board can take quadrature encoder output through ENCODER_A and ENCODER_B pin of J2. The interface is protected against ESD using the bidirectional TVS ESD protection diode ESD122. R6 and R15 are used as the pull-up resistors. R7, C8, R16 and C13 forms the low-pass noise filters on each line before feeding to the MCU GPIO pins.

The reference design can also take potentiometric analog voltage position feedback. In that case connect the analog voltage output from the potentiometric position sensor between ENCODER_A and GND. The pull-up resistor R6 may not be required in that case and depends on the position sensor used. If potentiometric feedback is used, configure the P1.4 (connecting the signal POT / ENC_A) port of the MCU as an ADC input.

# 3 Hardware, Software, Testing Requirements, and Test Results

## 3.1 Required Hardware and Software

### 3.1.1 Hardware

#### 3.1.1.1 Reference Design Board Connector Configuration

图 9 shows the connector configuration of this reference design, which features:

- Two-terminal input for power supply (J3): This pin is used to connect the input DC supply from the battery. The positive and negative terminals can be identified as shown in 图 9.
- Two-terminal output for motor winding connection: The phase output connections for connecting to the BDC motor winding marked as OUT1 and OUT2 as shown in 图 9.
- Three-pin connector J1: This connector is used for external UART communication interface. The RX and TX pins enable the communication with external master controller. The FAULT pin of this connector gives indication on any overcurrent fault in the system.
- Four-pin connector J5: This is the programming connector for the MSP430FR2433 MCU. The two-wire Spy-Bi-Wire protocol is used to program the MSP430FR2433.
- Two-pin connector J2: This connector interfaces the position feedback signals from the motor.

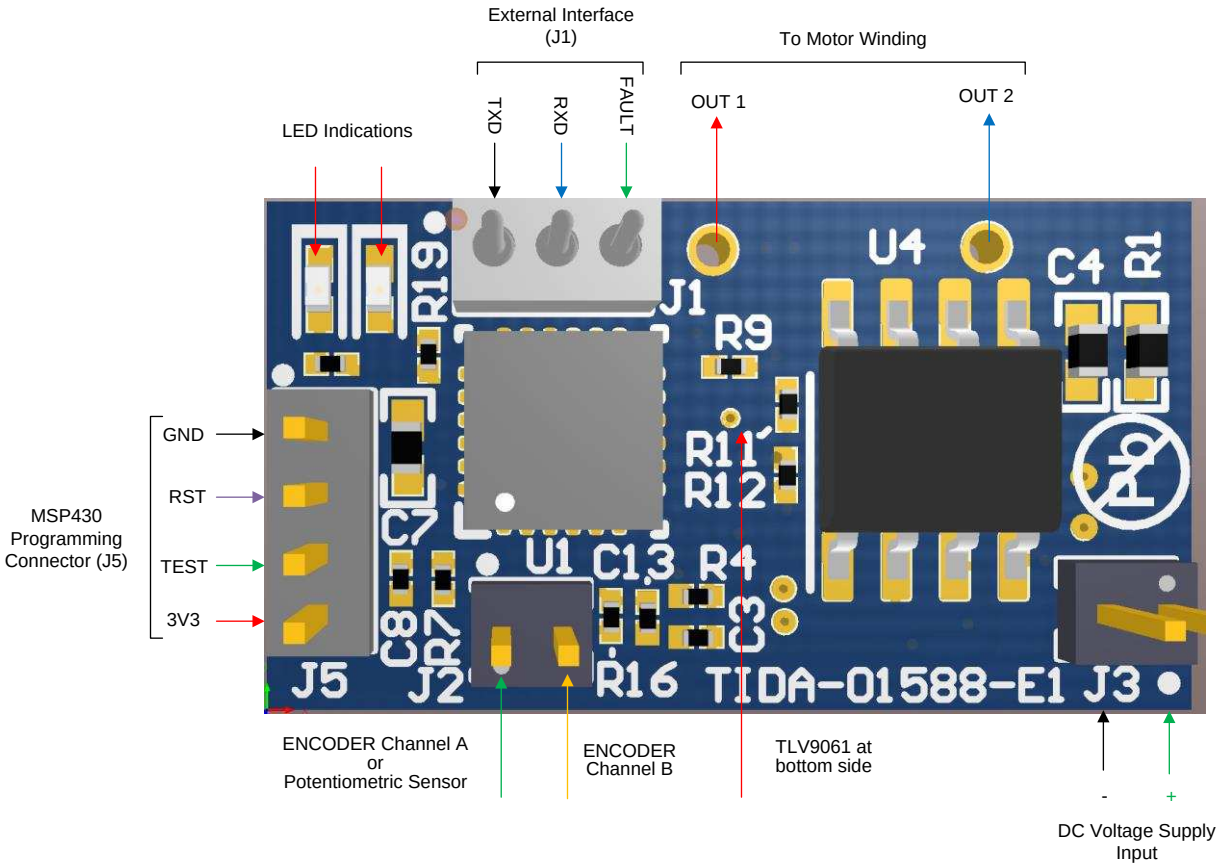


**图 9. PCB Connectors**

### 3.1.1.2 Programming the MSP430FR2433

The two-wire Spy-Bi-Wire protocol is used to program the MSP430FR2433 MCU. 图 10 shows the four-pin programming connector provided in the reference design board.

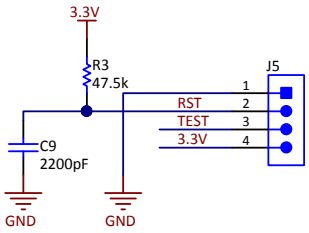




**图 10. Schematic of MSP430FR2433 Programming Connector**

See the development tools of the MSP430FR2433 for programming options with an external JTAG interface. Follow these steps to program the MSP430FR2433 MCU when the programming supply voltage is provided by the board itself:

1. Remove the motor connections from the board, and power on the input DC supply. Make sure that a minimum of 8-V DC input is applied and 3.3 V is generated in the board.
2. Connect the programmer to the board.
3. Open the Code Composer Studio™ (CCS) integrated development environment (IDE), and build and debug the code to program the MCU.

### 3.1.1.3 Procedure for Board Bring-up and Testing

Follow this procedure for board bring-up and testing:

1. Remove the motor connections from the board, and power on the input DC supply. Make sure that a minimum of a 8-V DC input is applied and the 3.3 V is generated in the board.
2. Program the MCU as detailed in 节 3.1.1.2. Make sure that the configuration in the program is done as per 节 3.1.2.
3. Remove the programmer, and switch off the DC input supply.
4. Connect the OUT1 and OUT2 outputs to the motor winding terminals.
5. Use a DC power supply with current limit protection and apply 8-V DC to the board. The motor will start rotating and stops at the position mentioned by the position reference.
6. To change direction, switch off the DC input, and correct the IN1 and IN2 logic in the program to reverse the direction of motor rotation and re-load the same in to the MCU.

### 3.1.2 Software

#### 3.1.2.1 High-Level Description of Application Firmware

The reference design's firmware offers the following features and user controllable parameters:

- Position control using feedback from a two-channel encoder
- Initialization of necessary PWM, ADC, and position feedback capture

表 3 lists the design's firmware system components.

**表 3. Firmware System Components**

| SYSTEM COMPONENT | DESCRIPTION |
|---|---|
| Development and emulation | Code Composer Studio version 7 |
| Target controller | MSP430FR2433 |
| PWM frequency | 20-KHz PWM (default), programmable for higher and lower frequencies |
| Interrupts | Port 1 Interrupts enabled on P1.4 and P1.5 corresponds to encoder interface. |
| PWM generation—timer configuration | IN1 – TA0.1; CLOCK = 16 MHz, OUTMOD_6, PWM frequency set for 20 KHz<br>IN2 – TA0.2; CLOCK = 16 MHz, OUTMOD_6, PWM frequency set for 20 KHz |
| Position feedback—encoder signals | P1.4 → ENCODER_CHANNEL A<br>P1.5 → ENCODER_CHANNEL B |
| ADC channel assignment | A4 → Potentiometric position feedback<br>A6 → DC bus voltage sensing<br>A7 → DC bus current sensing |
| MCU digital I/Os | P1.3 → Fault indication (LED2) |
| UART Communication | P2.5 → RX<br>P2.6 → TX |

#### 3.1.2.2 Customizing the Reference Code

Select the *main.c* file. Parameters exist at the top of the file that can be optimized and are included as the configuration variables. The following section of code shows these parameters:

#define PWM_PERIOD 400 // PWM Frequency (Hz) = 16MHz / ((2*PWM_PERIOD) - 1 )

#define DUTY_CYCLE 70 // Input Duty Cycle inversely relative to PWM_PERIOD

#define REF_ANGLE 90 // Reference angle for Position

#define ENC_RESOLUTION 2.6 //ENC_RESOLUTION (Encoder Resolution) = 360/Encoder pulses in 360 deg rotation

##### 3.1.2.2.1 PWM_PERIOD

PWM_PERIOD sets the value in capture and compare register 0 of Timer_A0. The Timer_A0 is initialized to operate at 16 MHz. Use 公式 6 to calculate the PWM frequency. The TIMER_A0 PWM is configured in up-down mode.

$$\text{PWM Frequency (Hz)} = \frac{16\ \text{MHz}}{((2 \times \text{PWM\_PERIOD}) - 1)} \tag{6}$$

For example, with PWM_PERIOD = 400, PWM Frequency ≈ 20 kHz

##### 3.1.2.2.2 DUTY_CYCLE

Adjust this parameter to control the speed of the motor. This parameter is inversely related to PWM_PERIOD.

##### 3.1.2.2.3 REF_ANGLE

REF_ANGLE sets the reference angle of the position reference, which means where to halt the motor.

##### 3.1.2.2.4 ENC_RESOLUTION

ENC_RESOLUTION value is calculated as per the number of encoder pulses. The reference design is tested with a motor having a two-channel encoder. Each channel gives 69 pulses in one complete 360° mechanical rotation. The pulses of encoder channel A and channel B are phase shifted. The total number of pulses (by counting both the channels) is 138. Because both of the channels produce phase-shifted pulses to form a quadratic encoder, the effective encoder position resolution (ENC_RESOLUTION ) can be calculated using 公式 7 as approximately 2.6°.

$$\text{ENC\_RESOLUTION} = \frac{360}{\text{Total encoder pulses in one mechanical rotation}} \tag{7}$$

#### 3.1.2.3 Running the Project in CCS

To run this project in CCS:

1. Install CCS and import the project *TIDA-01588_Firmware _V1.0*.
2. Read through 节 3.1.2.2 to customize the code.
3. Power up the board with an external supply as described in 节 3.1.1.2 and connect the programmer.
4. Build and debug the modified project to download the code to the MSP430FR2433.

## 3.2 Testing and Results

### 3.2.1 Test Setup

图 11 shows a representation of the test setup used in the lab to evaluate the TIDA-01588. The reference design is tested with a BDC motor that has the encoder position feedback.

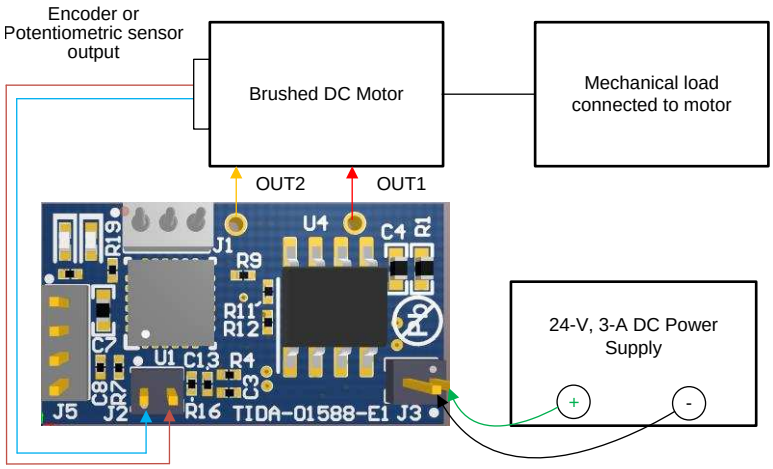


图 **11. Test Setup**

### 3.2.2 Power Supply Generated by the LDO—3.3-V

图 12 shows the 3.3 V generated from the LDO. The ripple in the 3.3-V rail is less than 15 mV.

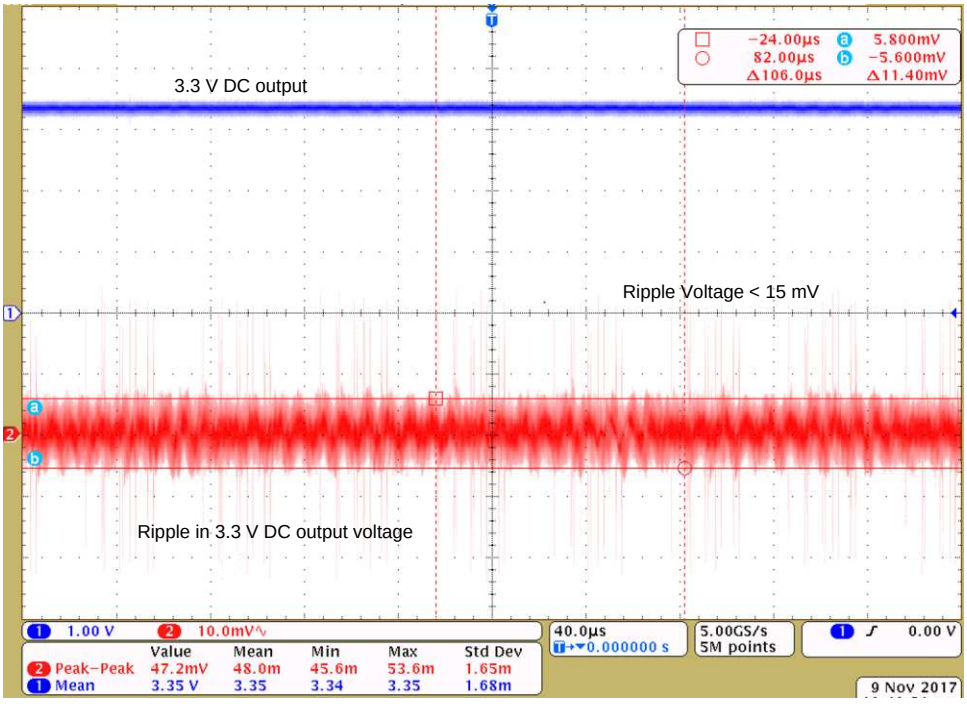


图 **12. 3.3 V Generated by TPS70933**

### 3.2.3 Testing of Current Sense Amplifier

#### *3.2.3.1 Current Sense Amplifier Transient Response*

The transient response of the current sense amplifier circuit with TLV9061 is observed by introducing step changes in voltage across the shunt resistor. The step change in sense voltage is created by switching the corresponding half bridge in the DRV8870, which causes the motor current to flow through the sense resistor.

图 13 shows the rising edge transient response of the current sense amplifier for a positive voltage drop across shunt resistor. The motor winding average current is approximately 750 mA. The transient response of the amplifier shows a settling time of approximately 1.5 µs to reach the final steady-state value within 5% dynamic error.

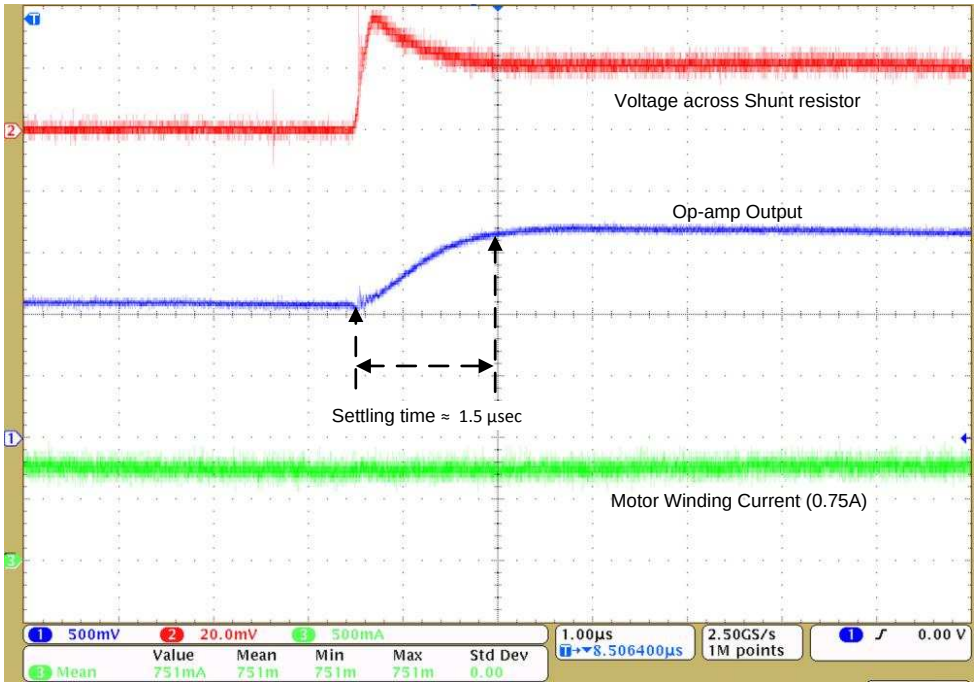


**图 13. Rising Edge Step Response of Current Sense Amplifier for Positive Current**

图 14 shows the falling edge transient response of the current sense amplifier for a positive voltage drop across shunt resistor. The motor winding average current is approximately 1.1 A. The transient response of the amplifier shows a settling time of approximately 1.6 µs to reach the final steady-state value within 5% dynamic error.

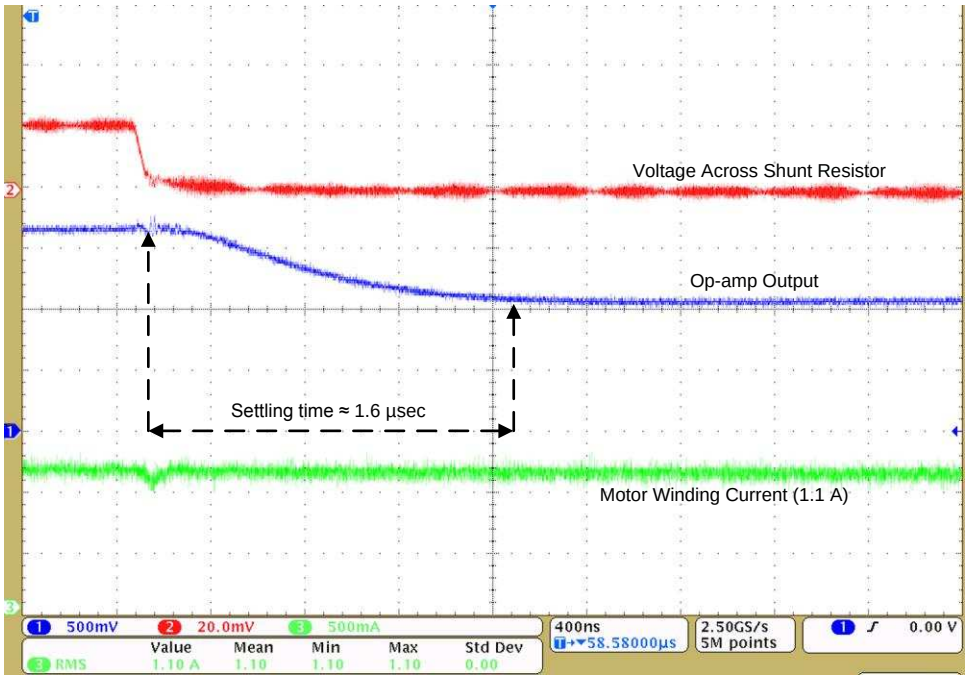


**图 14. Falling Edge Step Response of Current Sense Amplifier for Positive Current**

The high-gain bandwidth (10 MHz) of TLV9061 and the slew rate of 6.5 V/µs enable fast settling and a valid current sample even at low duty cycle. The amplifier has very good stability with good margin, and there is no observable unstable oscillations during transient response. The input EMI filter eliminate any external noise and provides robust performance.

#### 3.2.3.2 Current Sense Amplifier Transfer Function

图 15 shows the steady-state transfer function of the DC bus current through the 20-mΩ shunt resistor versus the output voltage of the TLV9061 amplifier. The output voltage equals 1.2 V when the DC bus current is zero. The transfer function is linear, which makes the software processing simple.

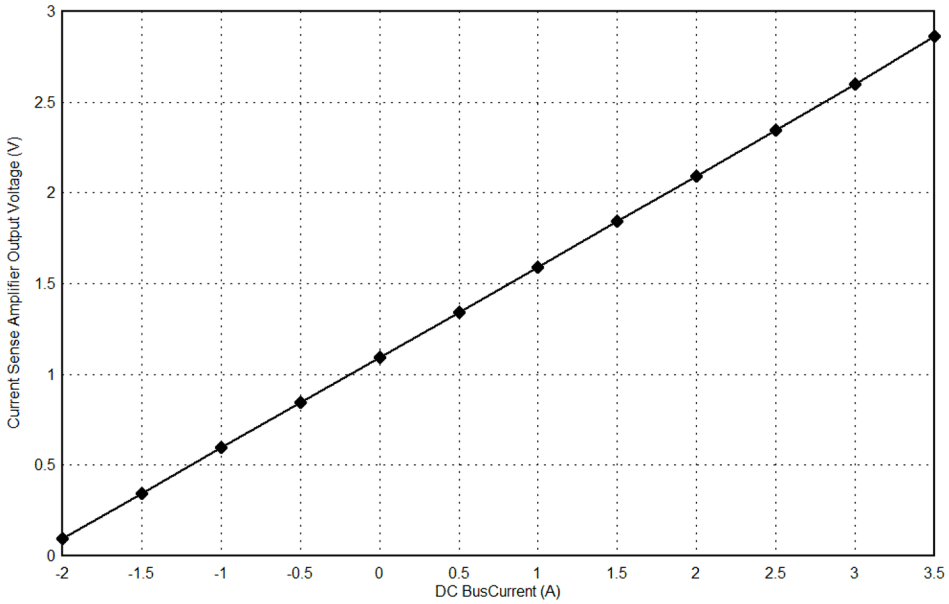


**图 15. DC Bus Current-Sensing Transfer Function**

### 3.2.3.3 DC Bus Current Sensing Accuracy

This test measures the DC accuracy of the current sense amplifier with a 20-mΩ sense resistor and TLV9061 configured as a single-ended differential amplifier at a gain of 24.95 V/V at 25°C ambient temperature. The full-scale DC bus current measurement range is –2 A to 3.5 A. The DC bus current is measured with a 6½ digit precision multimeter in series to the sense resistor and the output voltage of the current sense amplifier TLV9061 is measured with a 6½ digit precision multimeter. 图 16 shows the absolute error in DC bus current measurement. The uncalibrated absolute error remains within ±0.0.06 A with respect to the input current range from –2 A to 3.5 A. The uncalibrated error is dominated by sense resistor tolerance and offset voltage of opamp.. With op-amp offset voltage calibration, the absolute error reduces to less than ±0.015 A.

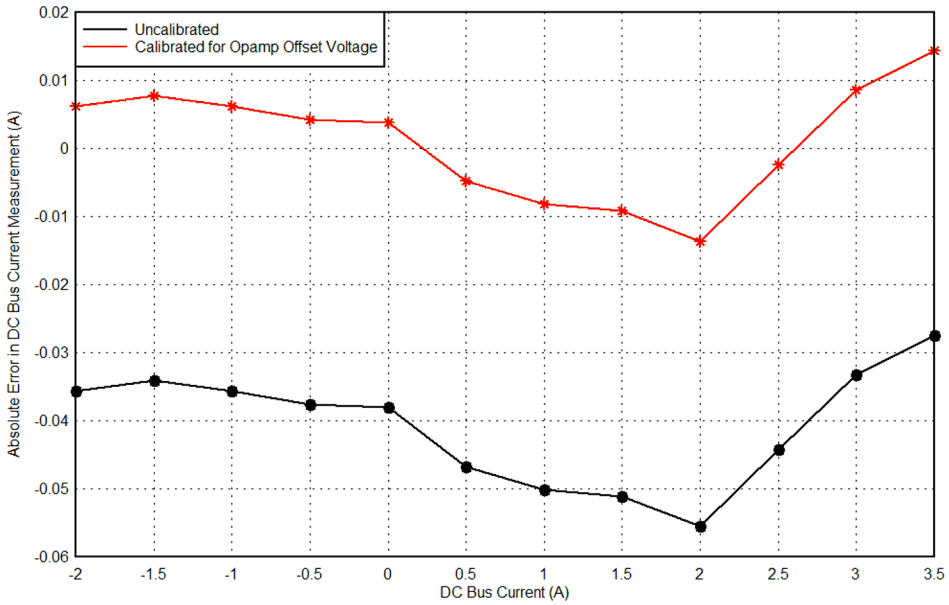


**图 16. Absolute Error in DC Bus Current Measurement**

图 17 shows the calibrated and uncalibrated relative error [%] in measured current from the op-amp output voltage. The calibrated relative error is less than 1%. The error can be further optimized by using the amplifier gain setting resistors and sense resistor with tight tolerance. The low error enables accurate current sensing and better torque performance from the motor drive.

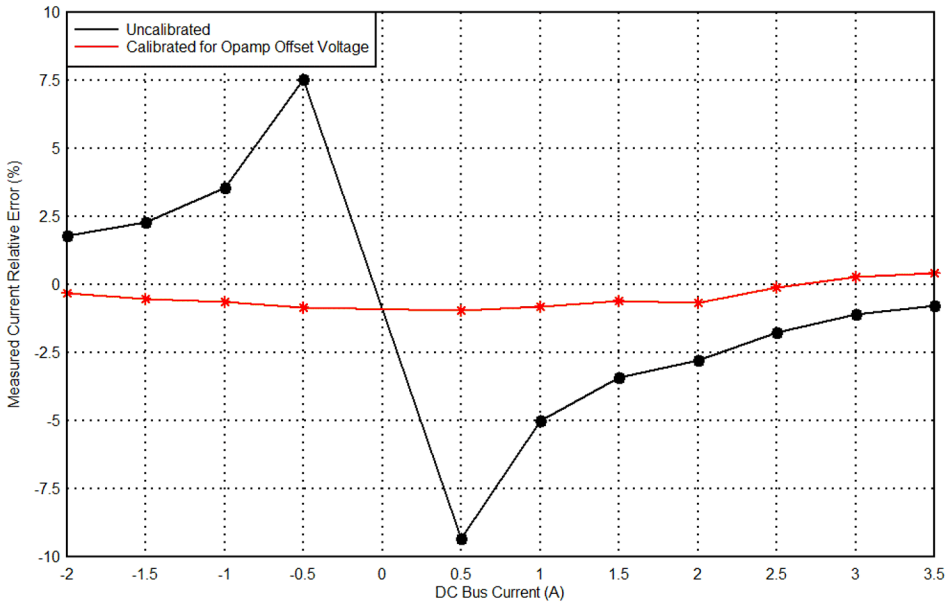


**图 17. Relative Error [%] in Measured Current From Amplifier Output Voltage**

### 3.2.4 Functional Testing of DRV8870

The DRV8870 has internal H-bridge power stage consists of four N-channel MOSFETs that are designed to drive current in the motor in both directions. The IN1 and IN2 signals are generated by the MCU, which control the states of DRV8870 drive voltage outputs OUT1 and OUT2 where the DC motor winding is connected. Refer to H-bridge control logic in *DRV8870 3.6-A Brushed DC Motor Driver (PWM Control) Data Sheet*[3].

图 18 shows the functional operation of DRV8870 at the following test conditions:

- IN1—25% PWM at 20-kHz switching frequency
- IN2—100% (High—3.3V)
- Input DC voltage = 10.8 V
- Winding current = 1.5-A RMS

OUT2 switches at approximately 75% pulse width at 20 kHz (when IN1 = 25%) and OUT1 is LOW always, as explained in *DRV8870 3.6-A Brushed DC Motor Driver (PWM Control) Data Sheet*[3].

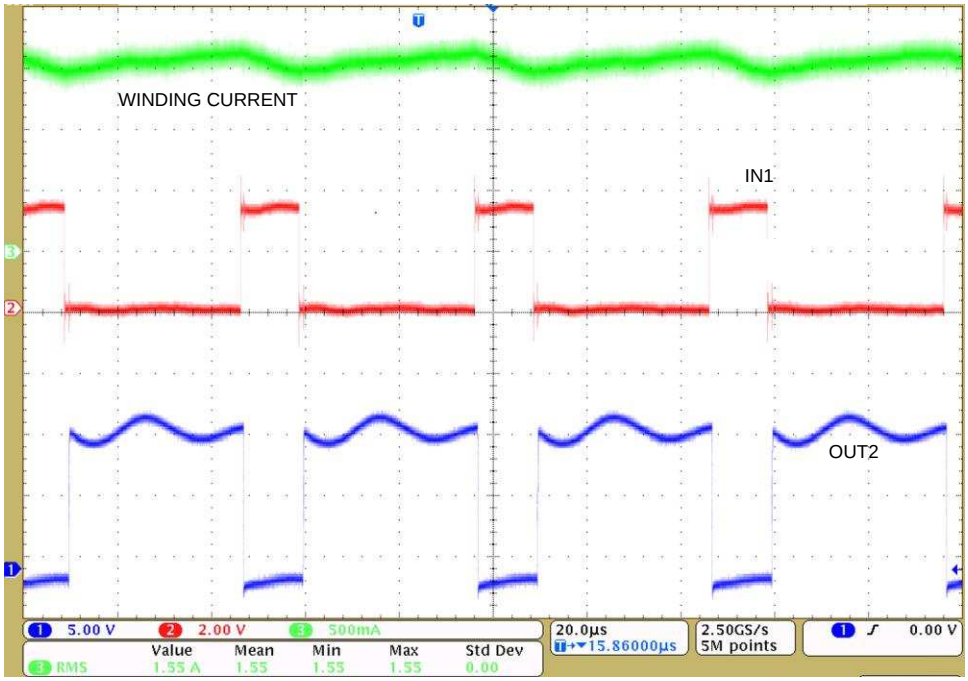


**图 18. DRV8870—Functional Evaluation**

### 3.2.5 Load Test

The load test is performed with a BDC motor at 10.8-V DC, and the motor is loaded to 1.4-A RMS. 图 19 shows motor winding current and the output voltage with 95% duty cycle. The maximum temperature observed on DRV8870 is 98°C after 10 minutes of continuous running. No airflow is used during testing. Considering 98°C temperature of DRV8870 being high at 25°C ambient temperature, a small chip size heat sink can be attached to take the current of 1.4 A to enable the operation even at 55°C ambient temperature.

表 **4. Load Test Results at 10.8-V DC, 95% Duty Cycle**

| INPUT DC VOLTAGE (V) | INPUT DC CURRENT (A) | WINDING CURRENT (RMS) (A) | INPUT POWER (W) | MAXIMUM TEMPERATURE ON DRV8870(°C) |
|---|---|---|---|---|
| 10.8 | 1.52 | 1.4 | 16.4 | 98 |

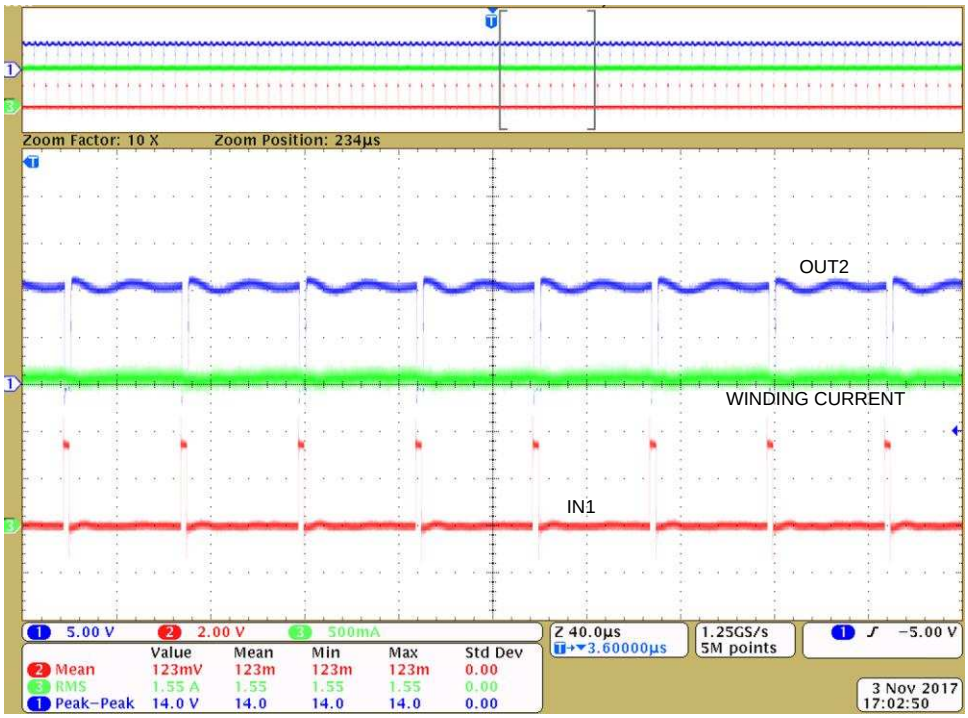


图 **19. Load Test Results at 10.8-V DC Input, 1.4-A RMS Winding Current, 95% Duty Cycle**

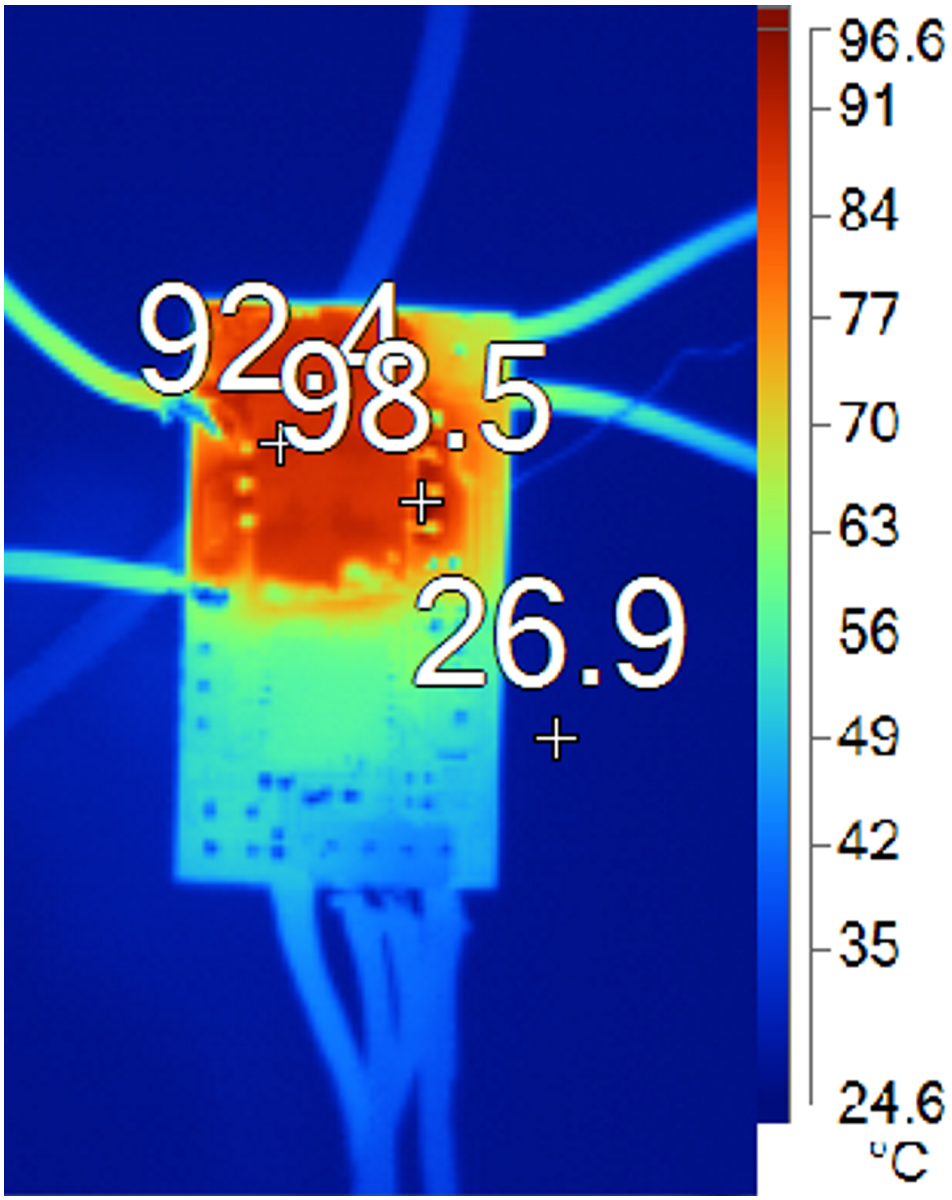


**图 20. Thermal Image at 10.8-V DC Input, 1.4-A RMS Winding Current, 95% Duty Cycle**

### 3.2.6 Load Test at Minimum and Maximum Voltages

The reference design can support a minimum DC input voltage of 6.5 V and a maximum input voltage of 25.2 V . 图 21 shows the test load test results at 6.5-V DC bus voltage and 1.5-A RMS motor current at 95% duty cycle. 图 22 shows the test load test results at 25.2-V DC bus voltage and 1.5-A RMS motor current at 95% duty cycle.

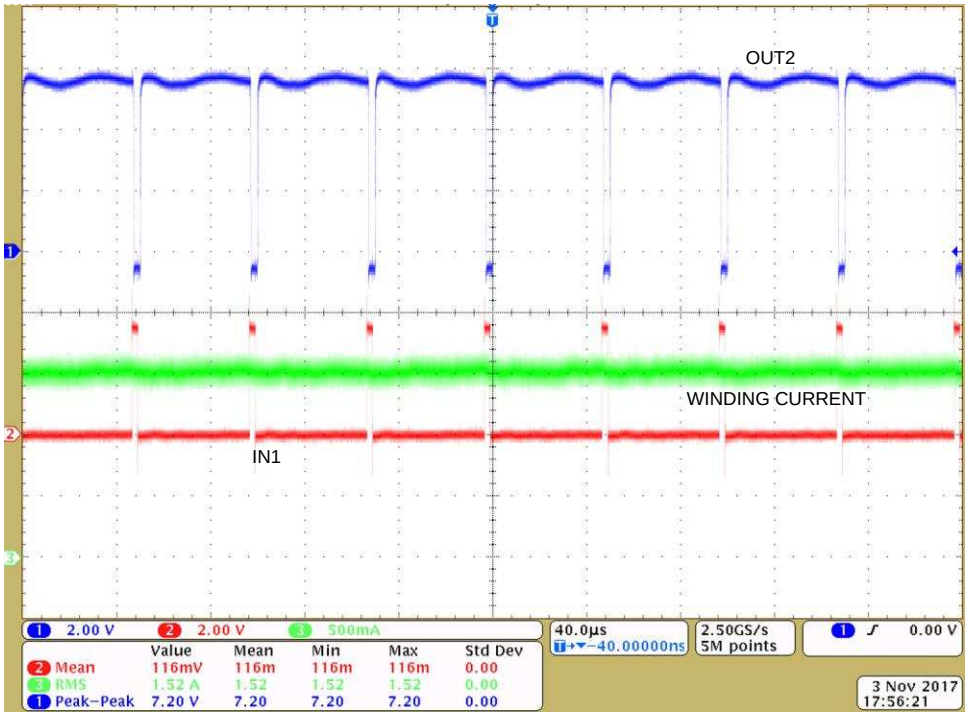


**图 21. Load Test Results at 6.5-V DC Input, 1.5-A RMS Winding Current, 95% Duty Cycle**

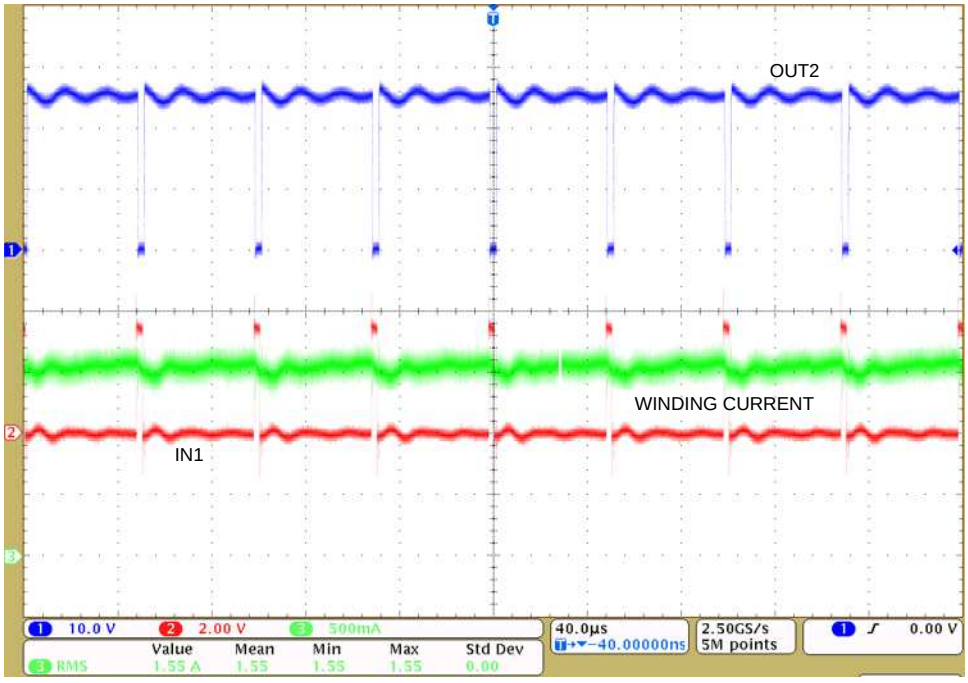


**图 22. Load Test Results at 25.2-V DC Input, 1.5-A RMS Winding Current, 95% Duty Cycle**

### 3.2.7 Power Stage Efficiency Test

The reference design board power stage efficiency is experimentally tested with a BDC motor load. 表 5 lists the test results without heat sink at a 100% duty cycle. 表 6 lists the test results without heat sink at a 95% duty cycle.

**表 5. Inverter Efficiency Test Results at 100% Duty Cycle Without Heat Sink and Without Airflow**

| INPUT DC VOLTAGE (V) | INPUT DC CURRENT (A) | INPUT DC POWER (W) | MOTOR WINDING RMS CURRENT(A) | BOARD OUTPUT POWER (W) | EFFICIENCY (%) |
|---|---|---|---|---|---|
| 10.79 | 0.1134 | 1.220 | 0.1083 | 1.161 | 95.14 |
| 10.76 | 0.2190 | 2.355 | 0.2138 | 2.270 | 96.41 |
| 10.85 | 0.3194 | 3.465 | 0.3172 | 3.348 | 96.62 |
| 10.79 | 0.4807 | 5.187 | 0.4800 | 4.986 | 96.12 |
| 10.80 | 0.6250 | 6.747 | 0.6201 | 6.446 | 95.54 |
| 10.83 | 0.7536 | 8.157 | 0.7490 | 7.732 | 94.79 |
| 10.80 | 0.8683 | 9.376 | 0.8635 | 8.820 | 94.07 |
| 10.86 | 1.0427 | 11.318 | 1.0380 | 10.496 | 92.74 |
| 10.80 | 1.2666 | 13.683 | 1.2612 | 12.484 | 91.24 |
| 10.87 | 1.4156 | 15.384 | 1.4104 | 13.912 | 90.43 |

**表 6. . Inverter Efficiency Test Results at 95% Duty Cycle Without Heat Sink and Without Airflow**

| INPUT DC VOLTAGE (V) | INPUT DC CURRENT (A) | INPUT DC POWER (W) | MOTOR WINDING RMS CURRENT(A) | BOARD OUTPUT POWER (W) | EFFICIENCY (%) |
|---|---|---|---|---|---|
| 10.84 | 0.1138 | 1.233 | 0.1145 | 1.169 | 94.78 |
| 10.79 | 0.1975 | 2.132 | 0.2027 | 2.040 | 95.67 |
| 10.78 | 0.3216 | 3.467 | 0.3338 | 3.332 | 96.10 |
| 10.82 | 0.4830 | 5.226 | 0.5039 | 4.984 | 95.38 |
| 10.87 | 0.5983 | 6.501 | 0.6266 | 6.165 | 94.83 |
| 10.82 | 0.7200 | 7.788 | 0.7548 | 7.320 | 93.99 |
| 10.79 | 0.8382 | 9.041 | 0.8797 | 8.408 | 93.00 |
| 10.82 | 1.0081 | 10.910 | 1.0596 | 10.011 | 91.76 |
| 10.78 | 1.2594 | 13.580 | 1.3247 | 12.296 | 90.54 |
| 10.75 | 1.4293 | 15.368 | 1.5050 | 13.801 | 89.80 |

The efficiency curve of these test conditions are plotted in 图 23.

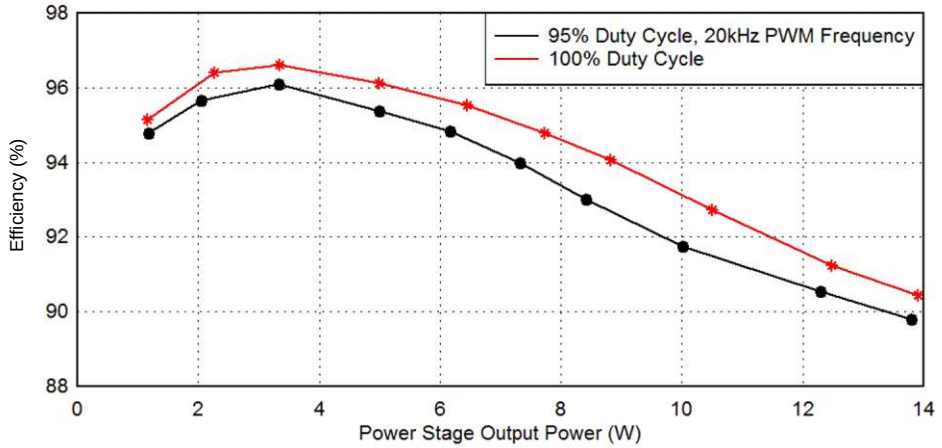


**图 23. Power Stage Efficiency Versus Output Power**

The low $R_{DS(ON)}$ of the motor driver DRV8870 ensure low power loss in the device and enable efficiency more than 90%. The exposed thermal pad of DRV8870 along with enough PCB copper area having multiple vias ensure efficient heat dissipation to the PCB. Refer to *DRV8870 3.6-A Brushed DC Motor Driver (PWM Control) Data Sheet*[3] to understand the power loss calculation and heat dissipation while designing with DRV8870.

### 3.2.8 Overcurrent Limit Results

The overcurrent limit is set by the voltage at the VREF pin of DRV8870 and the sense resistor value, which is explained in 节 2.3.2. For a fixed sense resistor value, the overcurrent limit can be set by adjusting the VREF voltage, which is done by modifying the resistor values of R10 and R5.

When overcurrent trip level (ITRIP) is reached, the device enforces slow current decay by enabling both low-side FETs. The device enforces slow current decay for a time of $t_{OFF}$ (typically 25 µs). After $t_{OFF}$ elapses, the output is re-enabled according to the two inputs, INx. The drive time ($t_{DRIVE}$) until reaching another ITRIP event heavily depends on the VM voltage, the back-EMF of the motor, and the inductance of the motor.

图 24 shows the overcurrent trip operation with a VREF = 0.35 V, using 20-mΩ sense resistor. Using the 公式 2, the expected overcurrent trip is 1.75 A, and the observed overcurrent trip is approximately 1.6 A.

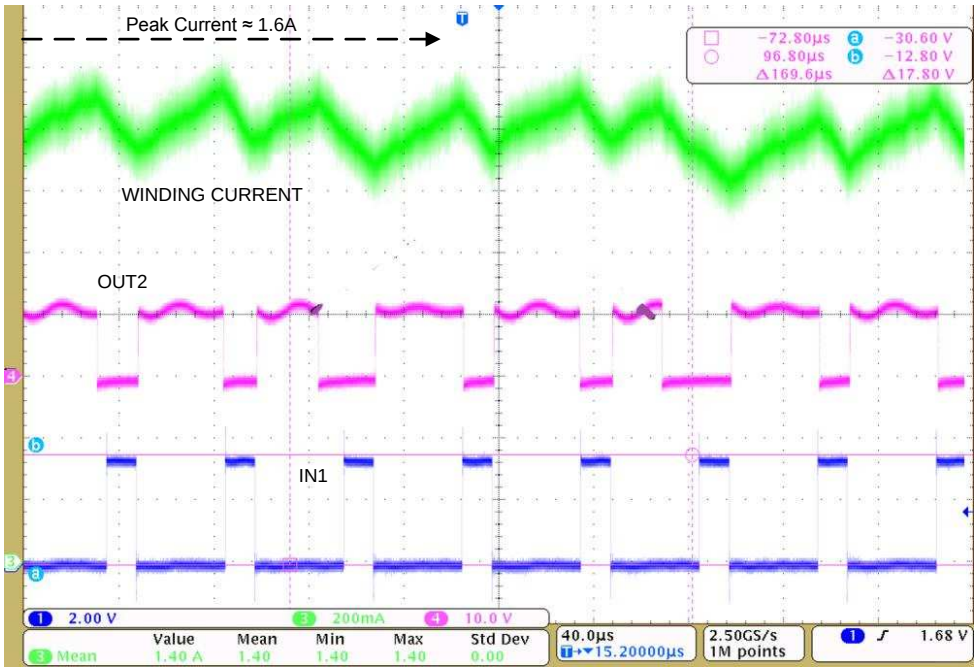


**图 24. Overcurrent Trip at VREF = 0.35 V With 20-mΩ Sense Resistor**

图 25 shows the overcurrent trip operation with a VREF = 0.55 V (R10 = 16.5 k, R5 = 3.3 k), using 20-mΩ sense resistor. The observed overcurrent trip is approximately 2.5 A.

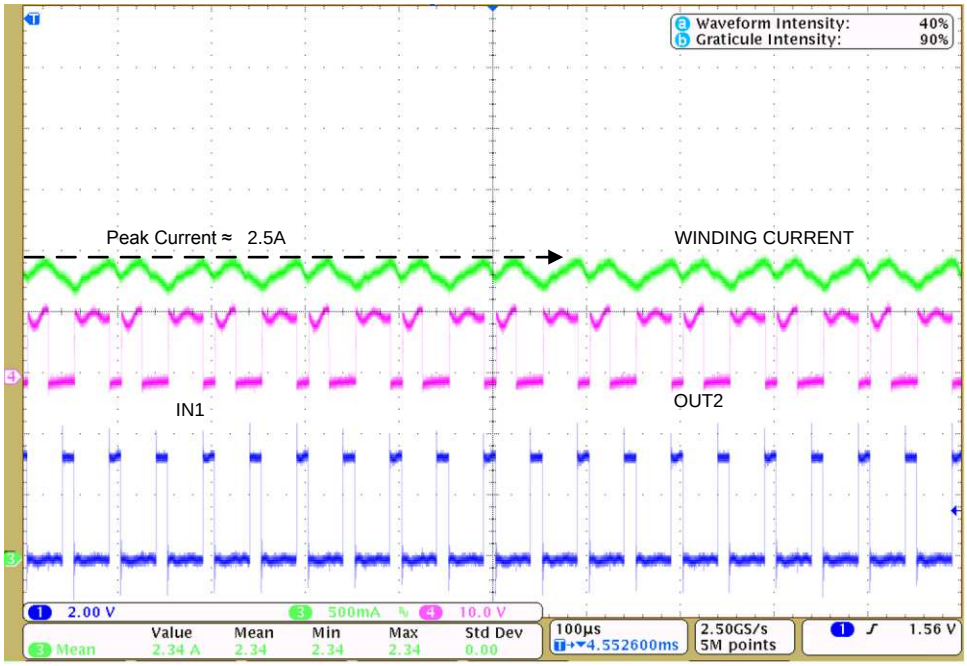


**图 25. Overcurrent Trip at VREF = 0.55 V With 20-mΩ Sense Resistor**

注: The error between the set current limit and observed current limit is less than 10%. The tolerance of the sense resistor, accuracy of set VREF voltage and tolerance in DRV8870 ISEN gain are the major contributors of current limit error. The error can be reduced by calibrating above mentioned factors.

### 3.2.9 Peak Current Test Results

图 26 shows the winding current of 2-A when the motor is stalled for more than 2 s.

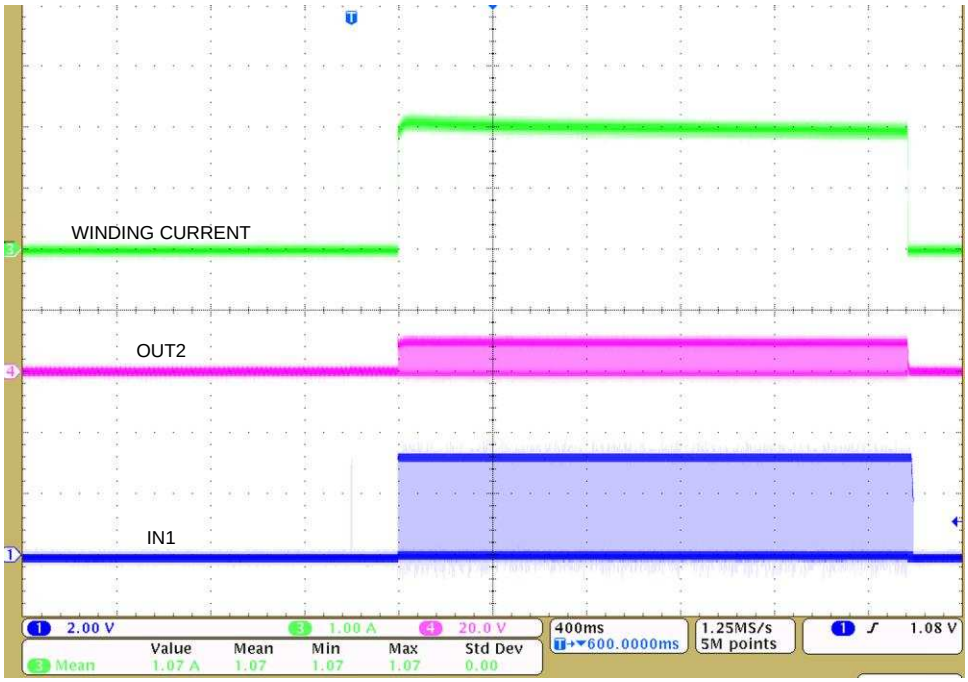


图 **26. Peak Current of 2-A in Motor Winding**

图 27 shows the thermal image of the board after 2 s. The maximum temperature observed on the DRV8870 is 89.7°C.

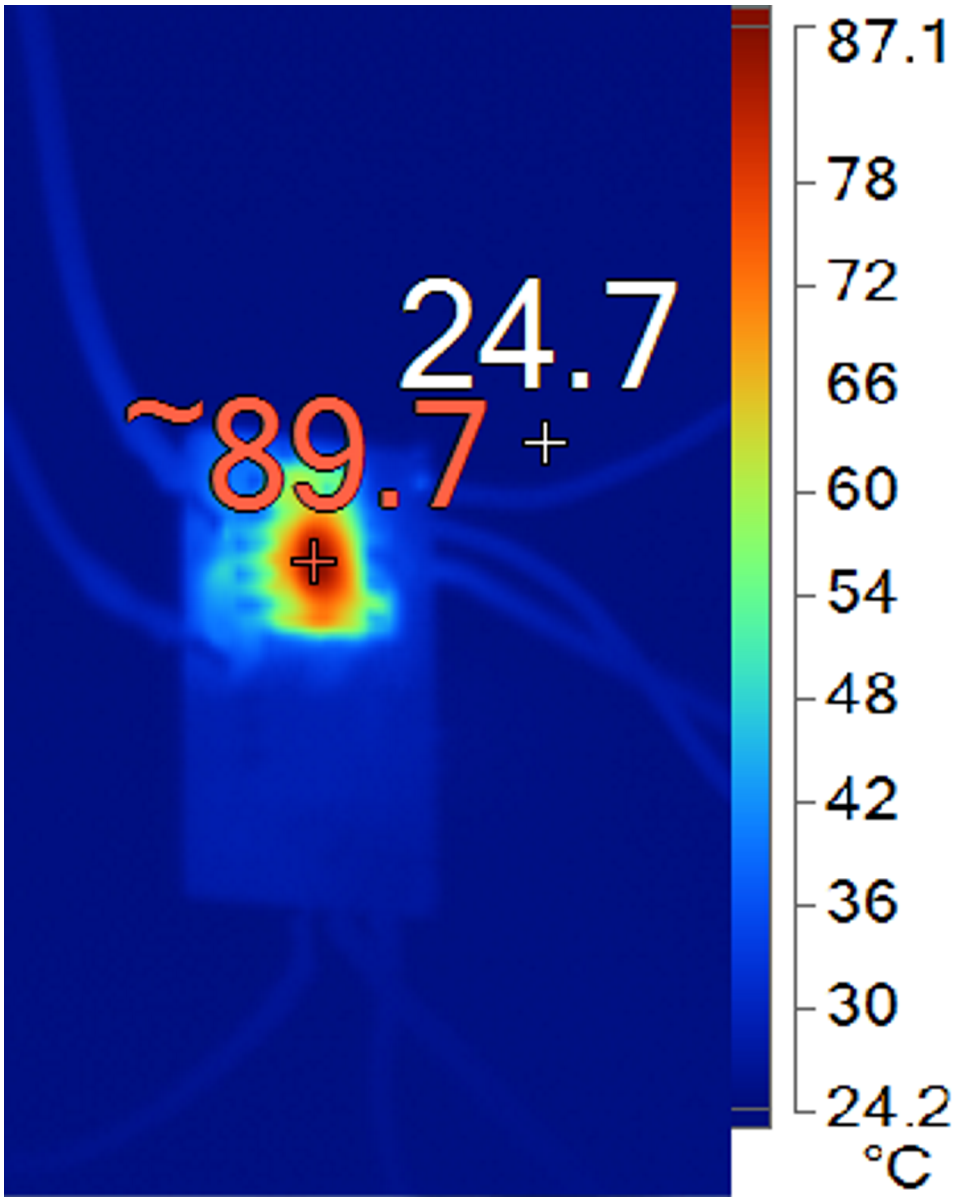


图 **27. Thermal Image of Board After 2 s With 2-A Peak Current in Motor Winding**

图 28 shows the winding current of 2.7 A when the motor is stalled for 1 s.

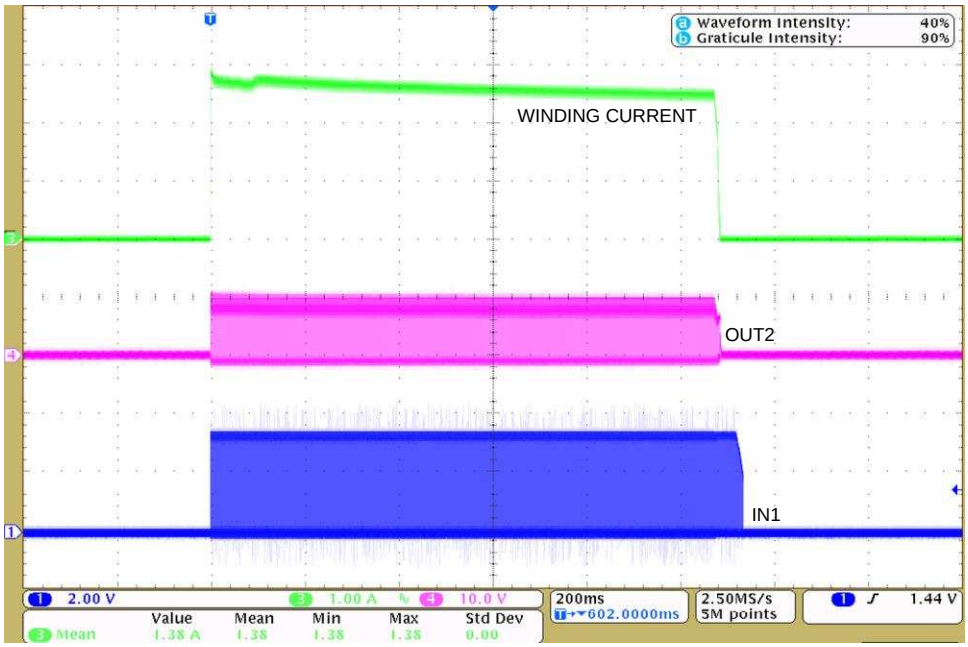


**图 28. Peak Current of 2.7 A in Motor Winding**

图 29 shows the thermal image of the board after 1 s. The maximum temperature observed on the DRV8870 is 92.1°C.

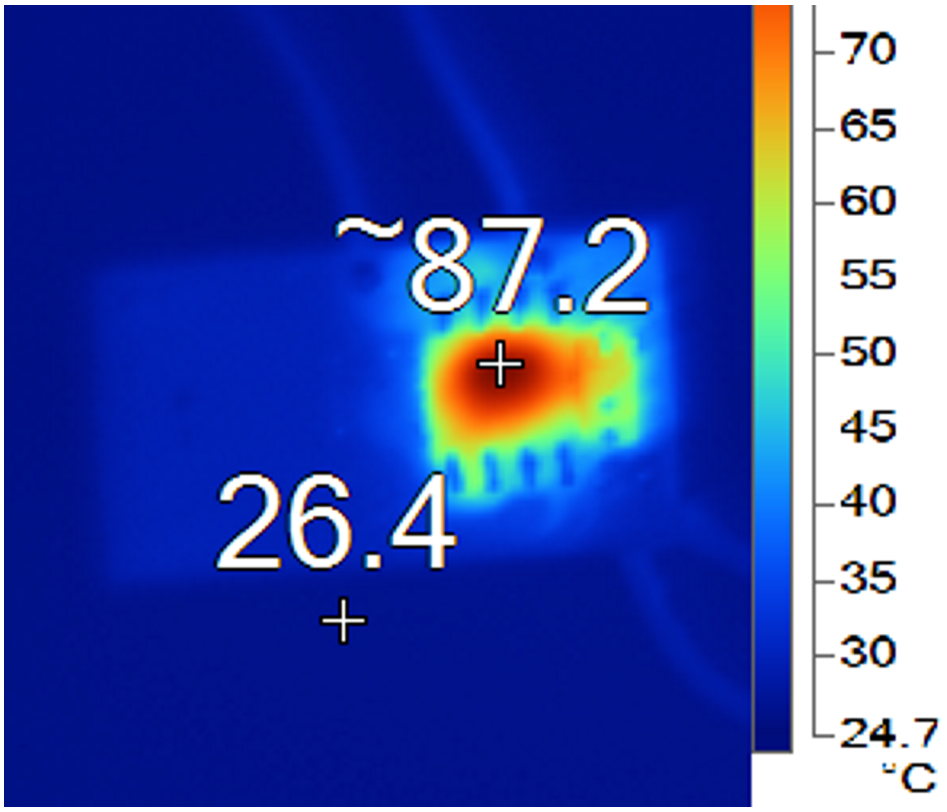


**图 29. Thermal Image of Board After 1 s With 2.7-A Peak Current in Motor Winding**

### 3.2.10 BDC Motor Position Control With TIDA-01588

The position control algorithm on MSP430FR2433 is implemented using port interrupts capability of the MCU. The testing is done on BDC motor which has inbuilt quadrature encoder. Each channel of quadrature encoder gives 69 pulses in one complete mechanical rotation of the motor. The resolution of the encoder interface can be calculated in 公式 7.

With this motor, the motor position can be measured up to 2.6° accurate and MCU is programmed accordingly. The testing was done to hold the motor position at 90° mechanical (¼ rotation) and 180° mechanical (half rotation) .

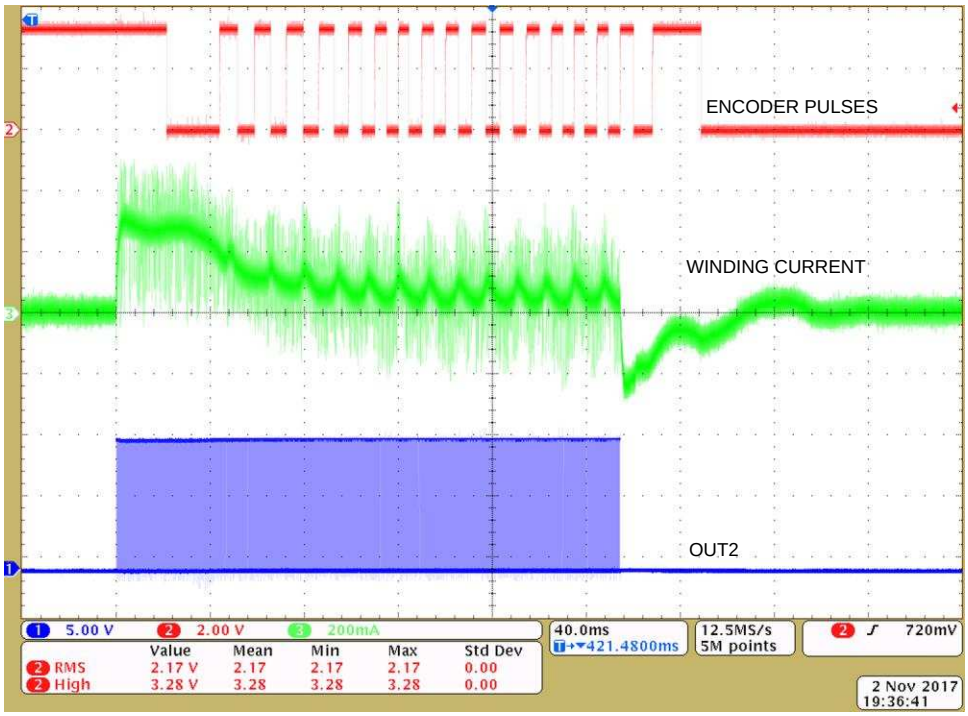


图 **30. Test Results for Position Control of Motor After One-Fourth Rotation**

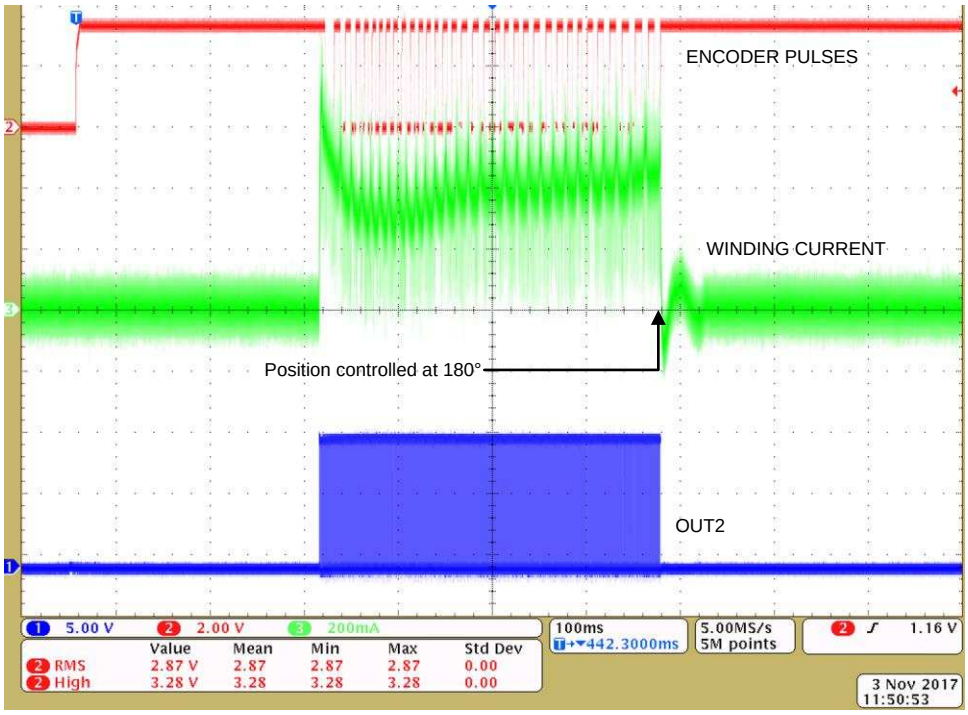


图 **31. Test Results for Position Control of Motor After Half Rotation**

# 4 Design Files

## 4.1 Schematics

To download the schematics, see the design files at TIDA-01588.

## 4.2 Bill of Materials

To download the bill of materials (BOM), see the design files at TIDA-01588.

## 4.3 PCB Layout Recommendations

The bulk capacitor for DRV8870 must be placed to minimize the distance of the high-current path through the motor driver device. The connecting metal trace widths must be as wide as possible, and numerous vias must be used when connecting PCB layers. These practices minimize inductance and allow the bulk capacitor to deliver high current. Small-value capacitors must be ceramic and placed closely to device pins. The high-current device outputs must use wide metal traces. The DRV8870 thermal pad must be soldered to the PCB top-layer ground plane. Multiple vias must be used to connect to a large bottom-layer ground plane. The use of large metal planes and multiple vias help dissipate the $I^2 \times R_{DS(ON)}$ heat that is generated in the device.

### 4.3.1 Layout Prints

To download the layer plots, see the design files at TIDA-01588.

## 4.4 Altium Project

To download the Altium project files, see the design files at TIDA-01588.

## 4.5 Gerber Files

To download the Gerber files, see the design files at TIDA-01588.

## 4.6 Assembly Drawings

To download the assembly drawings, see the design files at TIDA-01588.

# 5 Software Files

To download the software files, see the design files at TIDA-01588.

# 6 Related Documentation

1. Texas Instruments, *PowerPAD™ Thermally Enhanced Package Application Report*
2. Texas Instruments, *Current Recirculation and Decay Modes Application Report*
3. Texas Instruments, *DRV8870 3.6-A Brushed DC Motor Driver (PWM Control) Data Sheet*

## 6.1 商标



# 7 Terminology

BDC—Brushed DC motor

ESD—Electrostatic discharge

MCU—Microcontroller unit

PWM— Pulse width modulation

## 8 About the Author

**VARAD JOSHI** is a project trainee in the Industrial Systems team at Texas Instruments, where he is learning and developing reference design solutions with a focus on Motor drive systems. Varad is a final-year student pursuing a bachelor of engineering (B.E. hons) in electrical and electronics engineering from Birla Institute of Technology & Sciences (BITS), Pilani, Goa.

**MANU BALAKRISHNAN** is a systems engineer at Texas Instruments, where he is responsible for developing subsystem design solutions for the Industrial Motor Drive systems. Manu brings to this role his experience in power electronics and analog and mixed signal designs. He has system level product design experience in permanent magnet motor drives. Manu earned his bachelor of technology in electrical and electronics engineering from the University of Kerala and his master of technology in power electronics from National Institute of Technology Calicut, India.

**JASRAJ DALVI** is an End Equipment Lead with Industrial Systems team at Texas Instruments, where he is responsible for defining reference design solutions and control algorithms for motor control systems. He completed his Bachelors of Engineering degree in Electrical Engineering from University of Pune, India and his Post Graduate Diploma in Marketing Management at S.I.B.M. in Pune, India.

## 有关 TI 设计信息和资源的重要通知

德州仪器 (TI) 公司提供的技术、应用或其他设计建议、服务或信息，包括但不限于与评估模块有关的参考设计和材料（总称“TI 资源”），旨在帮助设计人员开发整合了 TI 产品的 应用； 如果您（个人，或如果是代表贵公司，则为贵公司）以任何方式下载、访问或使用了任何特定的 TI 资源，即表示贵方同意仅为该等目标，按照本通知的条款进行使用。

TI 所提供的 TI 资源，并未扩大或以其他方式修改 TI 对 TI 产品的公开适用的质保及质保免责声明；也未导致 TI 承担任何额外的义务或责任。TI 有权对其 TI 资源进行纠正、增强、改进和其他修改。

您理解并同意，在设计应用时应自行实施独立的分析、评价和 判断， 且应全权负责并确保 应用的安全性， 以及您的 应用 （包括应用中使用的所有 TI 产品）） 应符合所有适用的法律法规及其他相关要求。你就您的 应用声明，您具备制订和实施下列保障措施所需的一切必要专业知识，能够 (1) 预见故障的危险后果，(2) 监视故障及其后果，以及 (3) 降低可能导致危险的故障几率并采取适当措施。您同意，在使用或分发包含 TI 产品的任何 应用前， 您将彻底测试该等 应用 和该等应用所用 TI 产品的 功能而设计。除特定 TI 资源的公开文档中明确列出的测试外，TI 未进行任何其他测试。

您只有在为开发包含该等 TI 资源所列 TI 产品的 应用时， 才被授权使用、复制和修改任何相关单项 TI 资源。但并未依据禁止反言原则或其他法理授予您任何TI知识产权的任何其他明示或默示的许可，也未授予您 TI 或第三方的任何技术或知识产权的许可，该等产权包括但不限于任何专利权、版权、屏蔽作品权或与使用TI产品或服务的任何整合、机器制作、流程相关的其他知识产权。涉及或参考了第三方产品或服务的信息不构成使用此类产品或服务的许可或与其相关的保证或认可。使用 TI 资源可能需要您向第三方获得对该等第三方专利或其他知识产权的许可。

TI 资源系“按原样”提供。TI 兹免除对 TI 资源及其使用作出所有其他明确或默认的保证或陈述，包括但不限于对准确性或完整性、产权保证、无屡发故障保证，以及适销性、适合特定用途和不侵犯任何第三方知识产权的任何默认保证。

TI 不负责任何申索，包括但不限于因组合产品所致或与之有关的申索，也不为您辩护或赔偿，即使该等产品组合已列于 TI 资源或其他地方。对因 TI 资源或其使用引起或与之有关的任何实际的、直接的、特殊的、附带的、间接的、惩罚性的、偶发的、从属或惩戒性损害赔偿，不管 TI 是否获悉可能会产生上述损害赔偿，TI 概不负责。

您同意向 TI 及其代表全额赔偿因您不遵守本通知条款和条件而引起的任何损害、费用、损失和/或责任。

本通知适用于 TI 资源。另有其他条款适用于某些类型的材料、TI 产品和服务的使用和采购。这些条款包括但不限于适用于 TI 的半导体产品 (http://www.ti.com/sc/docs/stdterms.htm)、评估模块和样品 (http://www.ti.com/sc/docs/sampterms.htm) 的标准条款。

邮寄地址：上海市浦东新区世纪大道 1568 号中建大厦 32 楼，邮政编码：200122